

CUPP-99/1  
hep-ph/9901401  
January 1999

# NEW VARIABLES FOR NEUTRINO OSCILLATION DIAGNOSTICS AT SUPERKAMIOKANDE AND THE SUDBURY NEUTRINO OBSERVATORY

Debasish Majumdar <sup>1</sup> and Amitava Raychaudhuri <sup>2</sup>

*Department of Physics, University of Calcutta,  
92 Acharya Prafulla Chandra Road, Calcutta 700 009, India*

## ABSTRACT

The SuperKamiokande collaboration has presented results on the observation of solar neutrinos. The Sudbury Neutrino Observatory (SNO) is also expected to go on-line in the near future. We propose several new variables, insensitive to the absolute flux of the initial solar neutrino beam, which probe the shape of the observed spectrum at these experiments and can sensitively signal neutrino oscillations. One class of such variables involves normalised moments of the distributions recorded at the two facilities while another variable, specific to SNO, depends on the integrated charged and neutral current signals. The utility of these variables in the context of supernova neutrinos, both from the collapse epoch and the post-bounce era, is also emphasised. It is shown that, notwithstanding the imprecise nature of the information about the initial neutrino spectra from a supernova, oscillations can be detected using these variables and it will be possible to distinguish between the alternatives of oscillation to a sequential neutrino *vis-a-vis* that to a sterile neutrino.

PACS Nos.: 14.60.Pq, 26.65.+t, 97.60.Bw

---

<sup>1</sup>E-mail address: debasish@tnpdec.saha.ernet.in

<sup>2</sup>E-mail address: amitava@cubmb.ernet.in

# 1 Introduction

Neutrino physics has moved centrestage after the recent SuperKamiokande (SK) evidence in support of a non-zero neutrino mass and oscillation in their atmospheric  $\nu$  data [1]. A massive neutrino has vast implications in astrophysics and cosmology and also signals physics outside the Standard Model (SM) [2]. Further indications of neutrino mass and the determination of the complete mass spectrum are therefore awaited with much interest.

Historically, the long-standing solar neutrino problem [3] had offered the first glimpse of the oscillation of a  $\nu_e$  to a different neutrino. This oscillation partner state could be one of the sequential neutrinos,  $\nu_\mu$  or  $\nu_\tau$ . It could just as well be a sterile neutrino,  $\nu_s$ , which has no weak interactions. If produced by neutrino oscillations, the latter will completely escape the detectors. The inclusion of a fourth neutrino – sterile, in view of the LEP and SLC results – is suggested from the several evidences indicative of neutrino oscillations, namely, the solar neutrino puzzle, the atmospheric neutrino anomaly and the results of the LSND experiment [4], all of which cannot be accommodated together in a three neutrino framework [5].

New, high statistics results on solar neutrinos are just becoming available. The huge fiducial volume of the SuperKamiokande detector [6] has already enabled the accumulation of data at unprecedented rates [7], improving, and to a large extent, corroborating the earlier results on solar neutrinos. Another detector of comparable size, the Sudbury Neutrino Observatory (SNO) [8] is shortly expected to be operational. The latter experiment, because of its capability to detect neutrinos *via* both charged current (CC) as well as neutral current (NC) detection channels, will shed light on the nature of the other neutrino – sequential or sterile – involved in the oscillation explanation of the reduction of the solar neutrino flux from its “standard” value. The large data sample from these two experiments will provide an opportunity to examine signals for neutrino oscillation in novel manners.

An uncertainty in drawing conclusions from the solar neutrino data creeps in through the imperfect knowledge of the initial neutrino flux. Though the shape of

the neutrino spectra from the different reactions occurring in the sun (the  $p$ - $p$  chain, CNO cycle, *etc.*) are known precisely from weak interactions and nuclear physics, their relative and absolute normalisations depend on the physics and astrophysics within the sun and vary from one solar model to another [9, 10]. The Boron neutrinos – only which are seen at SK and SNO – are particularly sensitive with the absolute normalisation varying, for example, as  $T_c^{18}$ , where  $T_c$  is the solar core temperature. It is therefore of interest to formulate methods to decipher signatures of oscillation in the observed data which are independent of this imperfect knowledge of the normalisation of the initial flux.

In this work we examine in detail several variables which depend on (a) the normalised moments of distributions seen at SK and SNO and (b) on the ratios of the charged and neutral current signals at SNO [11]. Though these variables are sensitive to the precisely understood shape of the Boron-neutrino spectrum, they are independent of its absolute normalisation. The high statistics data from the new detectors make such a study feasible. We illustrate how the magnitudes of the above-mentioned variables (and their ratios) extracted from the data yield direct information on the neutrino mixing angles and mass splittings. We further show how the variables can be used to distinguish whether the  $\nu_e$  oscillates to a sequential neutrino or to a sterile one. Some similar ideas have also been advocated in ref. [12, 13] where the focus has been on the energy spectrum of the scattered electron neutrino at SNO, the MSW mechanism etc. In this work, we restrict ourselves to vacuum oscillations. At the present time the existing evidences for solar neutrino oscillations cannot clearly distinguish between the vacuum oscillation and MSW resonant flavour conversion alternatives. In the latter case, the expressions for neutrino oscillation probabilities that we use in this work will have to be appropriately modified [14].

The proposed variables can also serve as useful tools to examine neutrino signals from a supernova. Though, in this case, the shape of the initial neutrino flux is known less precisely, nonetheless, we show that in the event of oscillations the variables can assume values which are beyond the range that can be expected from this uncertainty.

Neutrinos are emitted from two distinct epochs of a supernova explosion. In the collapse phase, which occurs first, only  $\nu_e$  produced from electron capture are emitted while in the post-bounce era neutrinos of all three flavours are produced. The pure  $\nu_e$  nature of the collapse phase beam – like the solar neutrino case – holds some advantages but this is partially offset by the much smaller number compared to the neutrinos emitted in the post-bounce period. While the detection of the latter for a supernova within a 10 kpc distance is very likely, those from the former will be observable provided the explosion occurs within a distance of about 1 kpc. Some initial results on these issues have been reported earlier [15].

In the next section we introduce the variables which we propose and show how they can signal solar  $\nu$ -oscillations to a sequential or a sterile neutrino. In section 3 we consider supernova neutrinos and illustrate how the variables can be useful in that context. We end in section 4 with some discussions.

## 2 The new variables and solar neutrinos

In this section we introduce variables insensitive to the absolute normalisation of the initial flux which may be used as diagnostic tools for solar neutrino oscillations at SuperKamiokande and SNO. We consider the effect of  $\nu$ -oscillations on the solar neutrino spectrum as seen at these detectors and elaborate on the sensitivity of the new variables. We restrict ourselves to the two-flavour oscillation case. Mixing of more than two kinds of neutrinos will change the expressions for the oscillation probability in a well-known fashion. This can be readily incorporated but will introduce more parameters in the form of additional mixing angles and mass splittings.

## 2.1 Solar Neutrino Oscillations at SuperKamiokande and SNO

In the two-flavour case, the probability of an electron neutrino of energy  $E$  to oscillate to a neutrino of a different type,  $\nu_x$ , after the traversal of a distance  $L$  is:

$$P_{\nu_e \rightarrow \nu_x} = \sin^2(2\vartheta) \sin^2\left(\frac{\pi L}{\lambda}\right) \quad (1)$$

where  $\vartheta$  is the mixing angle.  $\lambda$  is the oscillation length given, in terms of the mass-squared difference  $\Delta$ , by:

$$\lambda = 2.47 \left(\frac{E}{\text{MeV}}\right) \left(\frac{\text{eV}^2}{\Delta}\right) \text{metre} \quad (2)$$

From probability conservation:  $P_{\nu_e \rightarrow \nu_e} = 1 - P_{\nu_e \rightarrow \nu_x}$ .

In the above,  $\nu_x$  can be either a sequential neutrino,  $\nu_\mu$  or  $\nu_\tau$ , or a sterile neutrino,  $\nu_s$ . The difference between these two cases will manifest itself at the detectors as follows. At SuperKamiokande the neutrinos are detected *via*  $\nu - e$  scattering. For the  $\nu_e$  there are contributions through both CC and NC weak interactions. If neutrino oscillations are operative then in case a sequential neutrino is produced it will contribute to the signal only through the NC interactions (roughly one sixth of the  $\nu_e$  case) while a sterile neutrino will be entirely missed by the detector. At SNO the electron neutrinos will be detected through (a) CC as well as (b) NC interactions. If oscillations to sequential neutrinos occur then the signal in (a) will be appropriately reduced while that in (b) will be unaffected. On the other hand if  $\nu_e$  oscillates to a sterile state then both the CC and NC signals will suffer depletions.

## 2.2 The variables $M_n$ and $r_n$

One set of variables, immune to the absolute normalisation of the initial flux, that we propose for the extraction of oscillation signals consists of  $M_n$ , the normalised  $n$ -th moments of the neutrino distributions observed at SK and SNO. Specifically,

$$M_n = \frac{\int N_i(E) E^n dE}{\int N_i(E) dE} \quad (3)$$

where  $i$  stands for SK or SNO. It is seen from the definition that the uncertainty in the overall normalisation of the initial neutrino flux cancels out from  $M_n$ .

If neutrino oscillations are operative then we have

$$N_{SK}(E) = f(E) \left\{ P_{\nu_e \rightarrow \nu_e}(E, \Delta, \vartheta) \sigma_{SK}^e(E) + P_{\nu_e \rightarrow \nu_\mu}(E, \Delta, \vartheta) \sigma_{SK}^\mu(E) \right\} \epsilon_{SK} N_{SK}^0 \quad (4)$$

for oscillation to any sequential neutrino, chosen to be  $\nu_\mu$  in the above. Here,  $f(E)$  stands for the initial Boron-neutrino fluence,  $\epsilon_{SK}$  for the detection efficiency which, for the sake of simplicity, is assumed to be energy independent, and  $N_{SK}^0$  for the number of electrons in the SK detector off which the neutrinos may scatter.  $\sigma_{SK}^e(E)$  is the  $\nu_e$  scattering cross-section with both NC and CC contributions whereas  $\sigma_{SK}^\mu(E)$  is the  $\nu_\mu$  cross-section obtained from the NC interaction alone.

If the solar neutrinos oscillate to a sterile neutrino then eq. (4) will be replaced by

$$N_{SK}(E) = f(E) P_{\nu_e \rightarrow \nu_e}(E, \Delta, \vartheta) \sigma_{SK}^e(E) \epsilon_{SK} N_{SK}^0 \quad (5)$$

The SuperKamiokande detector uses 32 ktons of light water in which electrons scattered by  $\nu_e$  – through both charged and neutral current interactions – are detected *via* Čerenkov radiation. The  $\nu_e - e^-$  scattering cross-section is  $\sigma_{SK}^e = 9.4 \times 10^{-44} \text{cm}^2 (E/10 \text{MeV})$  [16]. Electrons interact with the  $\nu_\mu$  only through neutral currents with a cross-section  $\sigma_{SK}^\mu = 1.6 \times 10^{-44} \text{cm}^2 (E/10 \text{MeV})$  [16].

Only the CC contributions are relevant at SNO for the determination of the spectrum and we get:

$$N_{SNO}^{c.c.}(E) = f(E) P_{\nu_e \rightarrow \nu_e}(E, \Delta, \vartheta) \sigma_{SNO}^{c.c.}(E) \epsilon_{SNO}^{c.c.} N_{SNO}^0 \quad (6)$$

$N_{SNO}^0$  is the number of deuteron nuclei in the SNO detector and  $\epsilon_{SNO}^{c.c.}$  represents the CC detection efficiency assumed to be independent of the energy. The above result is valid for oscillation to sequential as well as sterile neutrinos since neither of them can interact *via* the charged current.

The SNO detector has 1kton of  $D_2O$  and neutrinos are primarily detected through the charged and neutral current disintegration of the deuteron:  $\nu_e + d \rightarrow e^- + p + p$ ,  $\nu +$

$d \rightarrow \nu + p + n$ , respectively. The  $e^-$  in the CC reaction is identified through its Čerenkov radiation. The neutral current process is signalled by the detection of the neutron for which several methods are under consideration. Since the neutral current detection is calorimetric, only the integrated signal is measured through this channel. The shape of the signal is measured using the charged current process. For this cross-section we use  $\sigma_{SNO}^{c.c.} = 1.7 \times 10^{-44} \text{ cm}^2 (E - 1.44)^{2.3}$  where  $E$  is in MeV [17].

Some results for  $M_1$  and  $M_2$  are presented in Table 1 for different values of the mass splitting  $\Delta$  and the mixing angle  $\vartheta$ . Notice that at SNO, these variables cannot distinguish between the sequential and sterile neutrino alternatives (for a variable suited to this purpose,  $R_{SNO}$ , see the following sub-section). It is seen from Table 1 that at SuperKamiokande for the smaller mixing angle ( $\vartheta = 30^\circ$ ), for any  $\Delta$  the difference between the values of  $M_1$  (as well as  $M_2$ ) for the sequential and sterile neutrino cases does not exceed 5% but the variation from the no oscillation ( $\Delta = 0$ ) limit can be as large as 10%. Present data tend to favour a vacuum oscillation mixing angle close to maximal and in the  $\vartheta = 45^\circ$  case the ranges of variation of  $M_1$  and  $M_2$  are significantly larger and a distinction between the sequential and sterile alternatives ought to be possible. At SNO,  $M_1$  and  $M_2$  vary over larger ranges and, in particular, at  $\Delta = 0.6 \times 10^{-10} \text{ eV}^2$  and  $\vartheta = 45^\circ$ , which are the currently indicated values, it is as much as 15% for  $M_1$  and 20% for  $M_2$ .

In order to assess the merits of these variables, it needs to be noted first that for both the SNO CC and SK signals, what is experimentally measured using the Čerenkov technique is the energy of the outgoing electron. In the case of SNO, the large mass of the deuteron forces the electron to move in the direction of the incident neutrino. Further, since the recoiling hadrons are heavy, the electron's energy equals the incident neutrino energy less the threshold energy for the CC reaction, 1.44 MeV. For SK there is a unique correlation between the electron's energy and scattering angle with the neutrino energy. Thus the neutrino spectrum can be readily reconstructed from the measured electron energy for both experiments using the well-known cross-sections for the appropriate scattering process. The huge sizes of both detectors ensure that

the error in the final results will be dominated by systematic uncertainties. A careful analysis of the level of precision expected at these experiments has been done in ref. [12] and a few per cent can be considered as a safe estimate.

In Fig. 1 we present the contours of constant  $M_1$  in the  $\Delta - \vartheta$  plane for the SK sequential (1a), SK sterile (1b), and SNO (1c) cases. The symmetry of these contours with respect to the  $\vartheta = 45^\circ$  line is a consequence of eq. (1). Using these contours, a precise measurement of  $M_1$  will immediately constrain the parameters of the neutrino sector. It can also be seen that the choice  $\Delta = 0.6 \times 10^{-10}$  eV<sup>2</sup> and  $\vartheta = 45^\circ$  which is preferred by the current data lies in a region where  $M_1$  changes rather sharply. Thus  $M_1$  may allow a more precise determination of the oscillation parameters.

We have also examined the ratios

$$r_n = \frac{(M_n)_{SK}}{(M_n)_{SNO}} \quad (7)$$

Before discussing these variables we must make a cautionary remark that the inherent risks of drawing conclusions by combining the results from two different experiments with very different systematics should not be underestimated. Nonetheless, with high statistics data from both experiments, the variables  $r_n$  may be taken as indicative of the oscillation parameters.

In Fig. 2  $r_1$ ,  $r_2$ , and  $r_3$  are presented as a function of  $\Delta$  for two values of the mixing angle,  $\vartheta = 45^\circ$  and  $15^\circ$ . Note that around the preferred  $\Delta = 0.6 \times 10^{-10}$  eV<sup>2</sup> the distinction between the sequential and sterile neutrino cases is especially pronounced for the mixing angle of  $45^\circ$  and the variation of  $r_1$ ,  $r_2$ , and  $r_3$  from the no-oscillation reference value can be larger than 25%.

In Fig. 3 we present the contours of constant  $r_2$  in the  $\Delta - \vartheta$  plane for both the sequential and sterile neutrino cases while in Fig. 4 similar contours for  $r_3$  are shown. For both  $r_2$  and  $r_3$ , we have presented contours for two values of the variable larger than the no-oscillation limit while two are smaller. Notice that these contours alternate as a function of  $\Delta$  which is a reflection of the oscillating behaviour of  $r_{2,3}$  seen in Fig. 2. The sterile and sequential cases are especially different for the smallest values of  $\Delta$ .

### 2.3 The variable $R_{SNO}$

The SNO experiment will enable separate detection of the solar neutrinos through charged current and neutral current reactions of which the latter will only be a calorimetric measurement. As already noted,  $\nu_\mu$  or  $\nu_\tau$  produced as a result of oscillation will register at SNO *via* NC interactions with full strength but their energy will not permit charged current interactions. Therefore the ratio,  $R_{SNO}$ , of the total signal in the NC channel,  $\int N_{SNO}^{n.c.}$ , to the total (energy integrated) signal in the CC channel,  $\int N_{SNO}^{c.c.}$ , is a good probe for oscillations. Thus

$$R_{SNO} = \frac{\int N_{SNO}^{n.c.}}{\int N_{SNO}^{c.c.}} \quad (8)$$

where, for oscillation to a sequential neutrino,

$$\int N_{SNO}^{n.c.} = \int f(E) \sigma_{SNO}^{n.c.}(E) \epsilon_{SNO}^{n.c.} N_{SNO}^0 dE \quad (9)$$

in which  $\epsilon_{SNO}^{n.c.}$  is the detection efficiency for the NC channel and

$$\int N_{SNO}^{c.c.} = \int f(E) P_{\nu_e \rightarrow \nu_e}(E, \Delta, \vartheta) \sigma_{SNO}^{c.c.}(E) \epsilon_{SNO}^{c.c.} N_{SNO}^0 dE \quad (10)$$

It is obvious that  $R_{SNO}$  is independent of the absolute normalisation of the initial neutrino flux  $f(E)$  and depends only on its shape.

If oscillations to sterile neutrinos take place then eq. (9) is replaced by:

$$\int N_{SNO}^{n.c.} = \int f(E) P_{\nu_e \rightarrow \nu_e}(E, \Delta, \vartheta) \sigma_{SNO}^{n.c.}(E) \epsilon_{SNO}^{n.c.} N_{SNO}^0 dE \quad (11)$$

and eq. (10) is unchanged.

For the NC cross-section  $\sigma_{SNO}^{n.c.}$  we use  $0.85 \times 10^{-44} \text{cm}^2 (E - 2.2)^{2.3}$  where  $E$  is in MeV [17]. For simplicity, we have assumed  $\epsilon_{SNO}^{n.c.}$  to be independent of the energy and further equal to the efficiency of the CC reaction  $\epsilon_{SNO}^{c.c.}$ . If instead,  $\epsilon_{SNO}^{n.c.}/\epsilon_{SNO}^{c.c.} = r_\epsilon$  and it can be taken to be independent of the energy to a good approximation, then our results for  $R_{SNO}$  will be multiplied by this factor. The predictions can be improved by using more refined expressions for the NC and CC cross-sections and more realistic

inputs for detection efficiencies. Our purpose is to illustrate the utility of the proposed variables and we refrain from this exercise here.

Results for  $R_{SNO}$  for different values of the mass splitting  $\Delta$  are presented in Table 2 for three choices of the mixing angle  $\vartheta = 15^\circ, 30^\circ$  and  $45^\circ$ . In the absence of oscillations we find  $R_{SNO} = 0.382$ . Oscillation to sequential neutrinos decreases the denominator of eq. (8) while the numerator is unaffected. Thus  $R_{SNO}$  increases, very prominently for larger mixing angles, in this scenario. For sterile neutrinos both the NC and CC contributions are affected and we find little change in  $R_{SNO}$ . Thus,  $R_{SNO}$  will not be able to yield much information if oscillation to a sterile state is operative. A significantly different  $R_{SNO}$  from its no-oscillation limit will be a clear indication of oscillation to a sequential neutrino. In particular, for  $\Delta = 0.6 \times 10^{-10}$  eV $^2$  and  $\vartheta = 45^\circ$ ,  $R_{SNO}$  will be as high as 2.1 for oscillation to sequential neutrinos.

In Fig. 5, we present contours of constant  $R_{SNO}$  in the  $\Delta$ - $\vartheta$  plane for oscillation to sequential neutrinos. The symmetry of the contours about  $\vartheta = 45^\circ$  is expected. At  $\Delta = 0$  or  $\vartheta = 0^\circ$  or  $90^\circ$  the limit of no oscillations will be obtained. Values of  $R_{SNO}$  as high as 0.99 can only be achieved for smaller values of  $\Delta$ .

### 3 Supernova neutrinos and the new variables

SuperKamiokande and SNO will also serve as telescopes for neutrinos from supernova explosions. The detection of the SN1987A neutrinos gives us confidence that in the event of a supernova explosion both facilities will observe signals which will be pointing in the same direction and arrive at the same time. Here again, as for solar neutrinos, the proposed variables may be used to look for neutrino oscillations. The characteristic energy of the neutrinos being of the order of 10 MeV and the huge distance scales involved (several kpc) put the supernova in a unique position as a probe for oscillations governed by mass scales as small as  $10^{-18} - 10^{-19}$  eV $^2$ . We consider collapse phase and post-bounce era neutrinos in turn.

### 3.1 Collapse phase neutrinos

In the precursor to a supernova explosion the core of a massive star collapses under its own gravity once the nuclear burning stops and the pressure support from degenerate electrons is reduced due to electron capture. In this collapse phase, a burst of  $\nu_e$ , produced due to electron capture, is emitted in a timescale of about ten milliseconds. The burst stops when the density of the star becomes so large that neutrinos get trapped within. Though the number of neutrinos emitted in this phase is much less than that in the post-bounce era (see later), it has the advantage of being a pure electron neutrino beam. In this subsection we examine these neutrinos in the light of the new variables. The shape of the supernova neutrino spectra cannot be predicted with the precision of the solar case. We wish to establish that, nonetheless, the variables under discussion turn out to be useful in the search for neutrino oscillations.

In the event of a supernova explosion occurring sufficiently nearby (typically 1 kpc away) SK and SNO should detect a substantial number of neutrinos from the stellar core collapse phase [18, 19]. The collapse phase neutrino spectra from a realistic range of nuclear physics inputs as well as several stellar masses on the main sequence are presented in refs. [18, 19] and in the rest of our discussion in this subsection we use the neutrino spectrum presented there for a  $15M_\odot$  star at a distance of 1 kpc. If the supernova is much further away then the flux of neutrinos will be too weak to be detected with significant statistics.

We can readily adapt eqs. (3–6) to calculate the variables  $M_n$  for neutrinos from the collapse phase. It needs to be mentioned that supernova neutrinos have higher energy than in the solar case and small additional contributions to the SK and SNO signals will come from the CC and NC processes  $\nu_e + {}^{16}O \rightarrow e^- + {}^{16}F$  and  $\nu_x + {}^{16}O \rightarrow \nu_x + \gamma + X$  respectively which have thresholds of 15.4 MeV and 15.0 MeV. We have ignored these contributions and estimate that in this case their effect will not exceed about 10% of the signal.

$M_1$  and  $M_2$  for different values of  $\Delta$  are presented in Table 3 for maximal mixing ( $\vartheta = 45^\circ$ ). Results for oscillation to sequential and sterile neutrinos are separately

presented for SK. As noted for solar neutrinos, the SNO CC signal does not distinguish between these alternatives. The ratios  $r_1$  and  $r_2$  (see eq. (7)) are also presented in Table 3. It is seen from this Table that the variation in  $M_1$  can be 15% at both SK and SNO for some values of the oscillation parameters while for  $M_2$  it can be as large as 40% (25%) at SNO (SK). At SK, the variation is larger in the sterile neutrino scenario.

As mentioned earlier, unlike the solar neutrino case, the shape of the initial collapse phase neutrino spectrum is not precisely known and the above variation has to be set against the uncertainty in these variables which may arise, even in the absence of oscillations, from the imperfect knowledge of the initial neutrino flux. The neutrino energy spectrum receives contributions from electron capture on both free protons and heavy nuclei (in the  $fp$  shell). In ref. [18, 19] the abundance distribution of these are self-consistently determined with the evolution of thermodynamic conditions as collapse proceeds. As extreme conservative limits of the uncertainty in the neutrino spectrum we consider the situations where in one case the electron capture is only on free protons while in the other it is exclusively on heavy nuclei. Further, we estimate the uncertainties due to the unknown mass of the progenitor by considering a  $15M_\odot$  as well as a  $25M_\odot$  star. The results for  $M_1$ ,  $M_2$  as also  $r_1$ , and  $r_2$  for the above possibilities are presented in Table 4. It is seen from this Table that, in fact, the considered variation of the initial neutrino spectrum can lead to uncertainties in  $M_1$  and  $M_2$  larger than that due to oscillations which were presented in Table 3. Thus, for the collapse phase neutrinos,  $M_1$  and  $M_2$  cannot be used to unequivocally signal neutrino oscillations. The situation is somewhat better with the variables  $r_1$  and  $r_2$  in the sense that variation due to uncertainties in the initial spectrum can be at most 0.83 - 0.91 and 0.72 - 0.84 respectively and cannot mask an effect due to oscillations at least for some ranges of the mixing parameters. In Fig. 6, we present  $r_1$ ,  $r_2$ , and  $r_3$  as a function of  $\Delta$  for two values of the mixing angle  $\vartheta$ . Notice that around  $\Delta = 1 \times 10^{-18}$  eV<sup>2</sup> these variables can clearly distinguish between oscillation to a sequential or to a sterile neutrino for  $\vartheta = 45^\circ$ .

The variable  $R_{SNO}$  – eq. (8) – turns out to be very efficient to look for oscillations

in the collapse phase neutrino data. The variation of  $R_{SNO}$  with the mass splitting  $\Delta$  is shown in Table 5 where the mixing angle has been chosen to be  $\vartheta = 45^\circ$ . From these results it is seen that  $R_{SNO}$  can be increased several times if oscillation to sequential neutrinos occur and can achieve values as high as 1.7. It should be borne in mind that these results are for maximal mixing and there will be a suppression for other mixing angles. The sterile neutrino alternative affects the variable only marginally. The significance of the results presented in Table 5 can only be gauged once a comparison is made with the uncertainty in  $R_{SNO}$  due to the imprecise knowledge of the initial neutrino flux. In Table 6 results are presented for  $R_{SNO}$  in the absence of oscillations for both  $15M_\odot$  and  $25M_\odot$  stars. It is seen from this Table that the value of  $R_{SNO}$  is not sensitive to the typical examples of stellar collapse considered, which include combinations of initial conditions as reflected in the zero age main sequence mass of the pre-supernova star, matrix elements of the electron capture on heavy nuclei etc., and varies within the range 0.382 – 0.445. Therefore, if  $R_{SNO}$  is found to be very different from the predicted no-oscillation value then this difference cannot be attributed to the range of variations expected from astrophysical and nuclear physics grounds and will point towards oscillation to a sequential neutrino. In Fig. 7, we present contours of constant  $R_{SNO}$  in the  $\Delta - \vartheta$  plane for collapse phase neutrinos for oscillation to a sequential state. Notice that the highest values of  $R_{SNO}$  can be achieved only for smaller choices of  $\Delta$ .

### 3.2 Post-bounce epoch neutrinos

In the post-bounce epoch, thermal neutrinos and also anti-neutrinos of all three flavours are emitted on a time scale of a few seconds. The flux of these neutrinos is higher than those from the collapse phase and, indeed, is intense enough that neutrinos from this era of a supernova event at a distance of 10 kpc will register a statistically significant signal at SK and SNO. For example, the SN1987A explosion registered 11 and 8 events respectively at the smaller Kamiokande and IMB detectors. The sequence of arrival-times of these neutrinos can yield information on neutrino masses [20]. In contrast,

the discussion here, based on neutrino oscillations, will shed light on neutrino mass splittings.

The  $\tau$ - and  $\mu$ -type neutrinos and anti-neutrinos emitted during this era are pair-produced in the supernova and, in the absence of degeneracies, are predicted to have the same energy spectrum. The  $\nu_e$  and  $\bar{\nu}_e$  have different spectra and due to their additional charged current interactions inside the star have lower energy than the  $\nu_\mu$  and  $\nu_\tau$ . Neutrino oscillations between these states will therefore induce a complicated energy distribution of  $\nu$  and  $\bar{\nu}$  of different flavours [21]. In this sub-section we examine how the spectral shape variables, introduced earlier, can be utilised to discern oscillations in such a signal.

In the following analysis three different post-bounce neutrino spectra are at play; namely, those for the  $\nu_e$ , the  $\bar{\nu}_e$  and the  $\nu_x$  where the latter stands for neutrinos as well as anti-neutrinos of the  $\mu$  and  $\tau$  types. Here, for the purposes of illustration, we use the spectra extracted from the results presented in [22]. We restrict ourselves, as earlier, to two flavour vacuum neutrino oscillations. Since the  $\tau$ - and  $\mu$ -flavours are on an equal footing as far as the spectra and the detectors are concerned, we can consider mixing with any one of these as characteristic of oscillation to a sequential neutrino. Thus, for example, if we consider  $\nu_e \leftrightarrow \nu_\mu$  oscillations, then the  $\nu_\tau$  neutrinos and anti-neutrinos will be entirely unaffected while both neutrinos and anti-neutrinos of the electron and muon type undergo oscillations. Had we considered MSW resonant flavour conversion instead, then, depending on the sign of the mass squared difference, either the neutrinos or the anti-neutrinos would have undergone conversion.

Unlike the previously discussed solar and collapse phase neutrinos, here, for the first time, we have both neutrinos and anti-neutrinos of all three flavours in the initial beam. This adds several new features to the analysis. For example, while oscillations to sequential or sterile neutrinos affected the CC signal in the same manner in the earlier cases, this is no longer the case. Thus, for post-bounce neutrinos, oscillation to  $\nu_\mu$  results in some of the  $\nu_e$  changing to muon neutrinos but at the same time some electron neutrinos are produced from the  $\nu_\mu$  in the original beam. Since there are no

sterile neutrinos initially, the situation will be different if the  $\nu_e$  oscillates to a sterile state. Thus even *via* the CC interactions the two cases can be distinguished. Further at SNO, in addition to the NC interactions, the  $\bar{\nu}_e$  will register via the CC reaction  $\bar{\nu}_e + d \rightarrow e^+ + n + n$  which has a threshold of 4.03 MeV [17]. We have not included a small contribution from the process  $\bar{\nu}_e + {}^{16}O \rightarrow e^+ + {}^{16}N$ .

If we indicate the time integrated energy spectra of  $\nu_e$ ,  $\bar{\nu}_e$  and the neutrinos (and anti-neutrinos) of the  $\mu$  and  $\tau$  flavours by  $f^e(E)$ ,  $\bar{f}^e(E)$  and  $f^x(E)$  respectively then the observed signal at SK can be written as:

$$\begin{aligned}
N_{SK}(E) = & \left[ \left\{ f^e(E)P_{\nu_e \rightarrow \nu_e}(E, \Delta, \vartheta) + f^x(E)P_{\nu_\mu \rightarrow \nu_e}(E, \Delta, \vartheta) \right\} \sigma_{SK}^e(E) + \right. \\
& \left\{ f^e(E)P_{\nu_e \rightarrow \nu_\mu}(E, \Delta, \vartheta) + f^x(E)P_{\nu_\mu \rightarrow \nu_\mu}(E, \Delta, \vartheta) + f^x(E) \right\} \sigma_{SK}^\mu(E) + \\
& \left\{ \bar{f}^e(E)P_{\nu_e \rightarrow \nu_e}(E, \Delta, \vartheta) + f^x(E)P_{\nu_\mu \rightarrow \nu_e}(E, \Delta, \vartheta) \right\} \bar{\sigma}_{SK}^e(E) + \\
& \left. \left\{ \bar{f}^e(E)P_{\nu_e \rightarrow \nu_\mu}(E, \Delta, \vartheta) + f^x(E)P_{\nu_\mu \rightarrow \nu_\mu}(E, \Delta, \vartheta) + f^x(E) \right\} \bar{\sigma}_{SK}^\mu(E) \right] \epsilon_{SK} N_{SK}^0
\end{aligned} \tag{12}$$

for oscillation to any sequential neutrino, chosen to be  $\nu_\mu$  in the above. Here  $\bar{\sigma}_{SK}^x(E)$  is the  $\bar{\nu}_\mu$  or  $\bar{\nu}_\tau$  scattering cross-section off electrons which proceeds *via* the neutral current and is  $1.3 \times 10^{-44} \text{ cm}^2 E/(10 \text{ MeV})$ . For the  $\bar{\nu}_e$ , there is a charged current contribution so that the total  $\bar{\nu}_e - e$  scattering cross-section is  $3.9 \times 10^{-44} \text{ cm}^2 E/(10 \text{ MeV})$ .  $\bar{\sigma}_{SK}^e(E)$  receives an additional (dominant) contribution from the process  $\bar{\nu}_e + p \rightarrow e^+ + n$  which is  $9.4 \times 10^{-42} \text{ cm}^2 p_e E_e/(10 \text{ MeV})^2$  where  $p_e$  is the electron momentum and  $E_e = E - 1.3$  MeV its energy [16].

If instead, oscillations to a sterile neutrino are operative, then eq. (12) will be replaced by

$$\begin{aligned}
N_{SK}(E) = & [f^e(E)P_{\nu_e \rightarrow \nu_e}(E, \Delta, \vartheta)\sigma_{SK}^e(E) + 2f^x(E)\sigma_{SK}^\mu(E) \\
& + \bar{f}^e(E)P_{\nu_e \rightarrow \nu_e}(E, \Delta, \vartheta)\bar{\sigma}_{SK}^e(E) + 2f^x(E)\bar{\sigma}_{SK}^\mu(E)] \epsilon_{SK} N_{SK}^0
\end{aligned} \tag{13}$$

As discussed earlier, only the CC contributions are relevant at SNO for the extraction of the spectral shape and in this case the relevant formula valid for oscillation to

a sequential state is:

$$\begin{aligned}
N_{SNO}^{c.c.}(E) = & \left[ \left\{ f^e(E)P_{\nu_e \rightarrow \nu_e}(E, \Delta, \vartheta) + f^x(E)P_{\nu_\mu \rightarrow \nu_e}(E, \Delta, \vartheta) \right\} \sigma_{SNO}^{c.c.}(E) + \right. \\
& \left. \left\{ \bar{f}^e(E)P_{\nu_e \rightarrow \nu_e}(E, \Delta, \vartheta) + \bar{f}^x(E)P_{\nu_\mu \rightarrow \nu_e}(E, \Delta, \vartheta) \right\} \bar{\sigma}_{SNO}^{c.c.}(E) \right] \epsilon_{SNO}^{c.c.} N_{SNO}^0
\end{aligned} \tag{14}$$

while for oscillation to sterile neutrinos it is:

$$\begin{aligned}
N_{SNO}^{c.c.}(E) = & [f^e(E)P_{\nu_e \rightarrow \nu_e}(E, \Delta, \vartheta) \sigma_{SNO}^{c.c.}(E) + \\
& \bar{f}^e(E)P_{\nu_e \rightarrow \nu_e}(E, \Delta, \vartheta) \bar{\sigma}_{SNO}^{c.c.}(E)] \epsilon_{SNO}^{c.c.} N_{SNO}^0
\end{aligned} \tag{15}$$

In the above, we have only considered two flavour neutrino oscillations that involve the electron neutrino. This is because the SNO and SK detectors are primarily geared to look for the  $\nu_e$ . If two flavour oscillation occurs between the  $\nu_\mu \leftrightarrow \nu_\tau$  states then neither the SNO nor the SK signal will be affected at all. If  $\nu_\mu$  or  $\nu_\tau$  oscillates to a sterile state then though the SNO signal remains unchanged, there will, indeed, be a small depletion in the SK signal since the latter lacks the NC interaction of the sequential neutrino. We have not discussed this case since the effect will be small.

Some results for  $M_1$  and  $M_2$  for post-bounce epoch neutrinos are presented in Table 7 for different values of the mass splitting  $\Delta$  for the mixing angle  $\vartheta = 45^\circ$ . One major difference in this Table from those of the situations discussed earlier is that for post-bounce neutrinos SNO can distinguish between oscillation to sequential and sterile neutrinos. As noted earlier, this is because the post-bounce epoch beam has  $\nu_\mu$  and  $\nu_\tau$  components in addition to electron neutrinos. Since the spectra of the electron- and muon-type neutrinos are different, the net effect of oscillations is to change the CC signal by an amount different from that for the case of oscillation to sterile neutrinos. Due to the higher energy of the  $\nu_\mu$  and  $\nu_\tau$ , oscillation to sequential neutrinos always increases the signal at both SK and SNO while for the sterile case both larger and smaller values are possible depending on  $\Delta$ . It is seen from Table 7 that the effect of oscillations is most pronounced around  $\Delta = 1.2 \times 10^{-19}$  eV<sup>2</sup>. For example, for the sterile alternative, for  $M_1$  the deviation from the no-oscillation value is about 25% (20%) at SK (SNO) for  $M_2$  it is 45% (39%).

In order to gauge the utility of these variables, it needs to be first ascertained to what extent they are sensitive to changes in the input spectra of the neutrinos. These spectra are extracted from results on the evolution of supernova explosions and it is not easy to assess the range of uncertainty, *ab initio*. We consider as a conservative upper limit a variation of  $\pm 30\%$  in the absolute normalisation of each of  $f^e(E)$ ,  $\bar{f}^e(E)$ , and  $f^x(E)$ . In Table 8 are presented results for  $M_{1,2}$  and  $r_{1,2}$ , in the absence of oscillations, where independent variation of each spectrum in this range takes place. Notice that the variables are remarkably stable. Hence for neutrinos from the post-bounce epoch, the variables  $M_1$ ,  $M_2$ ,  $r_1$ , and  $r_2$  can be powerful tools to probe for oscillations.

In Fig. 8  $r_1$ ,  $r_2$ , and  $r_3$  are presented as a function of  $\Delta$  for two values of the mixing angle,  $\vartheta = 45^\circ$  and  $15^\circ$ . Notice that for oscillation to sequential neutrinos the variables are always smaller than the no oscillation limit while in the sterile case both larger and smaller values are possible. This difference can be attributed to the presence of the other sequential neutrinos in the parent beam.

In Fig. 9 we present the contours of constant  $r_2$  in the  $\Delta - \vartheta$  plane. For oscillation to sequential neutrinos, we have presented contours for four values of  $r_2$  which are all less than the no-oscillation limit as dictated by Fig. 8. In the sterile case, however, we have presented contours for two values of the variable larger than the no-oscillation limit while two are smaller. The vastly different nature of the contours for the sequential and sterile alternatives underscore the utility of these variables to pin-point the kind of oscillation at work.

For post-bounce epoch neutrinos the ratio,  $R_{SNO}$ , is also an effective probe for oscillations. In contrast, to the case of solar neutrinos, here it turns out to be sensitive to oscillations of an electron neutrino to a sterile state. As before,

$$R_{SNO} = \frac{\int N_{SNO}^{n.c.}}{\int N_{SNO}^{c.c.}} \quad (16)$$

where for oscillation to a sequential neutrino

$$\begin{aligned} \int N_{SNO}^{n.c.} = & \int [\{f^e(E) + 2f^x(E)\} \sigma_{SNO}^{n.c.}(E) \\ & + \{\bar{f}^e(E) + 2f^x(E)\} \bar{\sigma}_{SNO}^{n.c.}(E)] \epsilon_{SNO}^{n.c.} N_{SNO}^0 dE \end{aligned} \quad (17)$$

where to a good approximation the NC cross-section for anti-neutrinos of all flavours  $\bar{\sigma}_{SNO}^{n.c.}(E) = \sigma_{SNO}^{n.c.}(E)$  [17]. For the sterile neutrino alternative

$$\int N_{SNO}^{n.c.} = \int [\{f^e(E)P_{\nu_e \rightarrow \nu_e}(E, \Delta, \vartheta) + 2f^x(E)\} \sigma_{SNO}^{n.c.}(E) + \{\bar{f}^e(E)P_{\nu_e \rightarrow \nu_e}(E, \Delta, \vartheta) + 2f^x(E)\} \bar{\sigma}_{SNO}^{n.c.}(E)] \epsilon_{SNO}^{n.c.} N_{SNO}^0 dE \quad (18)$$

and

$$\int N_{SNO}^{c.c.} = \int N_{SNO}^{c.c.}(E) dE \quad (19)$$

where  $N_{SNO}^{c.c.}(E)$  is given by eq. (14) or eq. (15) depending on whether oscillation of electron neutrinos takes place to sequential or sterile neutrinos, respectively. In Table 9, we present  $R_{SNO}$  as a function of  $\Delta$  for  $\vartheta = 15^\circ$  and  $45^\circ$ . It is evident from this Table that  $R_{SNO}$  varies over a wide range (more than 100% of the reference no-oscillation value) in the sterile neutrino alternative while for oscillation to sequential neutrinos it is much less. Further, in the former case the effect of neutrino oscillations is always to increase  $R_{SNO}$  while for the latter the effect is in the opposite direction (barring for very small  $\Delta$ ).

To judge to what extent  $R_{SNO}$  is sensitive, in the absence of oscillations, to the initial neutrino spectra we have conservatively let these vary by  $\pm 30\%$ . These results, along with those where the variation is restricted to  $\pm 10\%$ , are presented in Table 10. Notice that a  $\pm 10\%$  variation in the initial flux can lead to values of  $R_{SNO}$  which can be achieved by oscillation to sequential neutrinos. On the other hand the range of variation obtained in the sterile neutrino alternative cannot be covered by even a  $\pm 30\%$  change in the initial flux. Therefore, we conclude that for the post-bounce epoch neutrinos  $R_{SNO}$  is a useful diagnostic tool only for oscillation to a sterile neutrino. In Fig. 10 are presented the contours of constant  $R_{SNO}$  in the  $\Delta - \vartheta$  plane for oscillation of the  $\nu_e$  to a sterile state. Note that the largest values of  $R_{SNO}$  can be achieved only for the small  $\Delta$  region.

## 4 Discussions and Conclusions

In this work we have elaborated on several variables that probe the shape of neutrino spectra seen at SK and SNO in a manner independent of the absolute normalisation of the neutrino fluence. The variables can be fruitfully used since the data from these experiments will be of unprecedented high statistics. As such they are useful to detect the modification of a neutrino spectrum by any process. Though, in this paper, we have illustrated their utility to signal two flavour vacuum neutrino oscillations only, similar analyses can be readily carried out for MSW resonant flavour conversion, multi-generational mixing, spin precession in a magnetic field, neutrino decay, *etc..* We hope to return to these issues in subsequent work.

One class of variables that was proposed in this work,  $M_n$ , are the normalised  $n$ -th moments of the observed neutrino spectra at SK and SNO and their ratios,  $r_n = (M_n)_{SK}/(M_n)_{SNO}$ . Another variable discussed in this paper,  $R_{SNO}$ , specific to SNO, is the ratio of the energy integrated NC signal to the energy integrated CC signal.

These variables are most appropriate for solar neutrinos. SuperKamiokande and SNO will be sensitive only to the so-called  ${}^8B$  neutrinos from the sun, the shape of whose energy spectrum is known precisely but the absolute normalisation is comparatively much less certain. (We have ignored a small contribution from *hep* neutrinos.) All the variables discussed in this work are independent of this absolute normalisation. We have found that  $M_1$  and  $M_2$  for the solar neutrinos will allow a distinction between the alternatives of oscillation of the  $\nu_e$  to sequential and sterile neutrinos. The related variables  $r_1$ ,  $r_2$ , and  $r_3$  can also be conveniently used to signal oscillations and distinguish between sequential and sterile neutrinos. Since oscillation to sterile neutrinos affect both the NC and CC signals at SNO in similar manners,  $R_{SNO}$  is rather insensitive in this case. It will be useful to detect oscillation to sequential neutrinos.

In addition to solar neutrinos, SK and SNO will also serve as neutrino telescopes for supernova explosions. The mass splitting  $\Delta$  that can be explored *via* supernova neutrinos  $\sim 10^{-18}$  or  $10^{-19}$  eV $^2$ , is, indeed, very tiny. The energy and length scales associated with supernova neutrinos provide a unique window for very small mass

splittings – a point noted earlier in ref. [23]. It has been speculated that oscillation of neutrinos from Active Galactic Nuclei or Gamma Ray Bursts will also be sensitive to such small  $\Delta$  [24].

Neutrinos are emitted at two stages of a supernova explosion. Though the earlier collapse phase neutrinos have the advantage of being a pure  $\nu_e$  beam, their flux is weaker and such an event will be detectable only if it occurs within a distance of 1 kpc. Unlike the solar case, there is also some uncertainty in the spectrum of the emitted neutrinos. We have found that due to these uncertainties it is not possible to unequivocally signal neutrino oscillations *via*  $M_1$  and  $M_2$ . However,  $R_{SNO}$  turns out to be a useful tool even in this case.

For the later post-bounce epoch, neutrinos and anti-neutrinos of all three flavours are emitted. In this case, we find that the variables  $M_1$ ,  $M_2$ ,  $r_1$ , and  $r_2$  are all suitable for probing neutrino oscillations. In the absence of oscillations, a variation of the initial spectra by as much as  $\pm 30\%$  is reflected by only a few per cent change in these parameters. In the post-bounce neutrino case,  $R_{SNO}$  turns out to be useful only for signalling oscillation to sterile neutrinos.

We conclude that the variables discussed in this work can be powerful diagnostic tools to search for neutrino oscillations in solar and supernova neutrino data obtained at SK and SNO. The results presented here can be further sharpened by simulating the detector geometries, acceptances, and detection efficiencies. These variables can also be used for other detectors – *e.g.* ICARUS which is sensitive only to  ${}^8B$  neutrinos from the sun – which are in the development stage.

## Acknowledgements

The authors are grateful to Sandhya Choubey for her help. This work is partially supported by the Eastern Centre for Research in Astrophysics, India. A.R. also acknowledges a research grant from the Council of Scientific and Industrial Research, India.

## References

- [1] Y. Fukuda *et al.*, (The Super-Kamiokande collaboration), *Phys. Rev. Lett.* **81**, 1562 (1998); T. Kajita, Talk at ‘*Neutrino ‘98*’, Takayama, Japan (1998).
- [2] Rabindra N. Mohapatra and Palash B. Pal, *Massive Neutrinos in Physics and Astrophysics, 2nd Ed.*, World Scientific, Singapore (1998).
- [3] B.T. Cleveland *et al.*, *Nucl. Phys. B(Proc. Suppl.)* **38**, 47 (1995); Kamiokande Collaboration, Y. Fukuda et al., *Phys. Rev. Lett.* **77**, 1683 (1996); GALLEX Collaboration, W. Hampel *et al.*, *Phys. Lett.* **B388**, 384 (1996); SAGE Collaboration, J.N. Abdurashitov *et al.*, *Phys. Rev. Lett.* **77**, 4708 (1996); J.N. Bahcall and M.H. Pinsonneault, *Rev. Mod. Phys.* **67**, 781 (1995).
- [4] LSND Collaboration, C. Athanassopoulos *et al.*, *Phys. Rev. Lett.* **75**, 2650 (1995); *ibid.* **77**, 3082 (1996); e-print nucl-ex/9706006.
- [5] S. Goswami, *Phys. Rev.* **D55** (1997) 2931; S. M. Bilenky, C. Giunti and W. Grimus, *Eur. Phys. J.* **C1** (1998) 247; e-print hep-ph/9711311.
- [6] Y. Totsuka, SuperKamiokande, Univ. of Tokyo Report No. ICRR-227-90-20 (1990).
- [7] Super-Kamiokande Collaboration, *Phys. Rev. Lett.* **81**, 1158 (1998); e-print hep-ex/9812011.
- [8] Sudbury Neutrino Observatory Proposal, Report No. SNO-87-12, (1987).
- [9] J.N. Bahcall, *Neutrino Astrophysics*, Cambridge Univ. Press (1989).
- [10] S. Turck-Chieze and I. Lopes, *Astrophys. J.*, **408**, 347 (1993); S. Turck-Chieze, S. Cahen, M. Casse and C. Doom, *ibid.*, **335**, 415 (1988).
- [11] A preliminary account has been presented in Debasish Majumdar and Amitava Raychaudhuri, e-print hep-ph/9812249 (submitted for publication).

- [12] J.N. Bahcall and E. Lisi, *Phys. Rev.* **D54**, 5417 (1996).
- [13] S.M. Bilenky and C. Giunti, *Phys. Lett.* **B311**, 179 (1993); *ibid.* **B320**, 323 (1994); G. Fiorentini, M. Lissia, G. Mezzorani, M. Moretti, and D. Vignaud, *Phys. Rev.* **D49**, 6298 (1994); W. Kwong and S.P. Rosen, *ibid.* **D51**, 6159 (1995).
- [14] Srubabati Goswami, Debasish Majumdar, and Amitava Raychaudhuri (*work in progress*).
- [15] Debasish Majumdar, Kamales Kar, Alak Ray, Amitava Raychaudhuri and Firoza K. Sutaria, e-print astro-ph/9807100 (submitted for publication).
- [16] Georg G. Raffelt, *Stars as Laboratories for Fundamental Physics*, The Univ. of Chicago Press (1996).
- [17] A.S. Burrows, in *Supernova*, A.G. Petschek (ed.) Springer-Verlag (1990). A more detailed exposition of neutrino-deuteron interactions can be found in J.N. Bahcall, K. Kubodera, and S. Nozawa, *Phys. Rev.* **D38**, 1030 (1988)
- [18] F.K. Sutaria and A. Ray, *Phys. Rev. Lett.* **79**, 1599 (1997).
- [19] F.K. Sutaria, Ph.D. dissertation, Univ. of Mumbai, Mumbai, India (1997).
- [20] See, for example, T. Totani, *Phys. Rev. Lett.* **80**, 2039 (1998); J.F. Beacom and P. Vogel, *Phys. Rev.* **D58**, 053010 (1998); *ibid.* **D58**, 093012 (1998).
- [21] For a discussion of the effect of oscillations on the signal at SK and SNO see, for example, Sandhya Choubey, Debasish Majumdar, and Kamales Kar, e-print hep-ph/9809424.
- [22] T. Totani, K. Sato, H.E. Dalhead and J.R. Wilson, *Astophys. J.* **496**, 216 (1998).
- [23] P. Reinartz and L. Stodolsky, *Z. Phys.* **27**, 507 (1985).
- [24] F. Halzen and D. Saltzberg, *Phys. Rev. Lett.* **81**, 4305 (1998).

Table 1:  $M_1$  and  $M_2$  for solar neutrinos for different values of the mass splitting  $\Delta$  for the SuperKamiokande and SNO detectors. For the former, results are presented for oscillation to sequential as well as sterile neutrinos. For SNO the two cases yield the same value of  $M_n$ . Two choices of the mixing angle  $\vartheta = 30^\circ$  and  $45^\circ$  have been considered.

$\Delta$ in $10^{-10}$ $\text{eV}^2$	$M_1$						$M_2$					
	$\vartheta = 30^\circ$			$\vartheta = 45^\circ$			$\vartheta = 30^\circ$			$\vartheta = 45^\circ$		
	SK		SNO	SK		SNO	SK		SNO	SK		SNO
	seq.	st.		seq.	st.		seq.	st.		seq.	st.	
.0	8.49	8.49	9.35	8.49	8.49	9.35	76.3	76.3	91.4	76.3	76.3	91.4
.3	8.76	8.83	9.62	8.89	9.03	9.76	80.8	82.1	96.3	83.0	85.3	98.8
.6	8.73	8.87	9.81	9.01	9.77	10.67	80.9	83.6	100.5	86.31	101.0	117.5
.9	7.85	7.57	8.52	7.34	6.57	7.09	65.7	61.2	77.4	57.4	44.8	53.1
1.2	8.13	8.02	8.67	7.94	7.74	8.21	69.3	67.2	78.4	65.7	61.9	69.4
1.5	8.71	8.78	9.36	8.82	8.93	9.37	79.2	80.0	90.6	80.6	82.0	90.1
1.8	8.79	8.88	9.75	8.94	9.10	9.95	81.8	83.5	98.6	84.6	87.5	102.2
2.1	8.66	8.71	9.76	8.75	8.85	10.02	80.0	81.2	100.1	82.1	84.5	105.5
2.4	8.47	8.46	9.45	8.46	8.44	9.52	76.3	76.3	94.4	76.3	76.4	96.7
2.7	8.26	8.18	9.02	8.12	7.95	8.74	72.2	70.7	85.6	69.6	66.6	80.8
3.0	8.34	8.29	8.99	8.25	8.15	8.72	73.1	72.0	84.1	71.3	69.1	78.6
3.5	8.54	8.56	9.37	8.57	8.59	9.38	77.0	77.2	91.2	77.4	77.8	91.1
4.0	8.61	8.65	9.56	8.67	8.75	9.69	78.6	79.3	95.8	79.9	81.3	98.5
4.5	8.45	8.44	9.35	8.43	8.40	9.36	75.8	75.6	92.1	75.4	75.1	92.5
5.0	8.45	8.44	9.23	8.43	8.41	9.14	75.4	75.1	88.9	74.8	74.2	87.1
5.5	8.48	8.47	9.29	8.47	8.46	9.26	75.9	75.8	90.1	75.7	75.4	89.2
6.0	8.53	8.54	9.41	8.55	8.57	9.46	77.0	77.3	92.8	77.4	77.9	93.7

Table 2:  $R_{SNO}$  for solar neutrinos for different values of the mixing angle,  $\vartheta$ , and the mass splitting,  $\Delta$ . Results are presented for oscillation to sequential as well as sterile neutrinos.

$\Delta$ in $10^{-10}$ eV $^2$	$R_{SNO}$					
	$\vartheta = 15^0$		$\vartheta = 30^0$		$\vartheta = 45^0$	
	Sequential	Sterile	Sequential	Sterile	Sequential	Sterile
0.0	0.382	0.382	0.382	0.382	0.382	0.382
0.3	0.422	0.384	0.532	0.389	0.613	0.392
0.6	0.480	0.383	0.991	0.387	2.117	0.396
0.9	0.467	0.378	0.848	0.362	1.428	0.337
1.2	0.438	0.380	0.623	0.375	0.788	0.370
1.5	0.422	0.383	0.537	0.387	0.620	0.390
1.8	0.417	0.383	0.512	0.386	0.577	0.388
2.1	0.431	0.383	0.582	0.387	0.706	0.390
2.4	0.444	0.382	0.660	0.383	0.873	0.384
2.7	0.444	0.380	0.658	0.375	0.867	0.370
3.0	0.444	0.381	0.659	0.379	0.869	0.377
3.5	0.431	0.382	0.582	0.381	0.705	0.380
4.0	0.434	0.383	0.597	0.386	0.735	0.388
4.5	0.435	0.382	0.606	0.381	0.753	0.380
5.0	0.440	0.382	0.634	0.381	0.813	0.381
5.5	0.437	0.382	0.614	0.381	0.770	0.381
6.0	0.434	0.382	0.597	0.382	0.735	0.382

Table 3:  $M_1$ , and  $M_2$  for collapse phase neutrinos for different values of the mass splitting  $\Delta$  for the SK and SNO detectors. For the former, results are presented for oscillation to sequential as well as sterile neutrinos. For SNO, the two cases yield the same value of  $M_n$ . The ratios  $r_1$  and  $r_2$  are also presented. The mixing angle  $\vartheta$  has been chosen to be  $45^\circ$ .

$\Delta$ in $10^{-18}$ eV $^2$	$M_1$			$r_1$		$M_2$			$r_2$	
	SK		SNO	seq.	st.	SK		SNO	seq.	st.
	seq.	st.				seq.	st.			
.0	13.3	13.3	16.1	0.83	0.83	202.4	202.4	281.7	0.72	0.72
.6	11.3	9.9	13.9	0.81	0.71	152.3	120.6	234.0	0.65	0.52
1.2	13.5	13.6	15.6	0.87	0.87	203.1	203.3	256.5	0.79	0.79
1.8	13.9	14.2	17.5	0.79	0.81	223.9	232.3	328.8	0.68	0.71
2.4	12.7	12.4	14.9	0.85	0.83	182.0	172.9	243.2	0.75	0.71
3.0	13.5	13.5	16.0	0.84	0.84	204.2	205.0	272.8	0.75	0.75
4.0	13.3	13.3	16.1	0.83	0.83	201.1	200.1	284.6	0.71	0.70
5.0	13.4	13.4	16.1	0.83	0.83	203.3	203.7	280.3	0.73	0.73
6.0	13.3	13.3	16.2	0.82	0.82	202.1	201.9	283.5	0.71	0.71

Table 4:  $M_1$ ,  $M_2$ ,  $r_1$ , and  $r_2$  in the absence of oscillations for collapse phase neutrino spectra obtained by changing the parameters for the progenitor star.

Progenitor	15M <sub>⊕</sub>						25M <sub>⊕</sub>					
	M <sub>1</sub>		r <sub>1</sub>	M <sub>2</sub>		r <sub>2</sub>	M <sub>1</sub>		r <sub>1</sub>	M <sub>2</sub>		r <sub>2</sub>
	SK	SNO		SK	SNO		SK	SNO		SK	SNO	
Combined	13.3	16.1	.83	202	282	.72	13.3	15.9	.84	200	275	.73
Only Free protons	15.9	17.5	.91	270	321	.84	14.9	16.8	.89	241	300	.81
Only Heavy nuclei	9.1	10.4	.87	89	118	.75	8.9	10.3	.87	86	115	.75

Table 5:  $R_{SNO}$  for collapse phase neutrinos as a function of the mass splitting  $\Delta$  for  $\vartheta = 45^\circ$ . Results are presented for oscillation to sequential as well as sterile neutrinos.

$\Delta$ in $10^{-18}$ eV $^2$	$R_{SNO}$	
	sequential	sterile
0.0	.431	.431
0.3	.844	.441
0.6	1.704	.419
0.9	1.356	.419
1.2	.833	.431
1.5	.661	.434
1.8	.708	.434
2.1	.890	.433
2.4	1.014	.427
2.7	.990	.427
3.0	.886	.430
3.5	.797	.433
4.0	.843	.431
4.5	.901	.430
5.0	.959	.434
5.5	.950	.435
6.0	.769	.430
6.5	.903	.432

Table 6:  $R_{SNO}$  for collapse phase neutrinos in the absence of oscillations for different neutrino spectra obtained by changing the parameters of the progenitor star.

Progenitor	Spectrum		
	Combined	only free protons	only heavy nuclei
$15M_{\odot}$	0.431	0.445	0.384
$25M_{\odot}$	0.431	0.440	0.382

Table 7:  $M_1$  and  $M_2$  for post-bounce epoch neutrinos for different values of the mass splitting  $\Delta$  for the SK and SNO detectors. Results are presented for oscillation to sequential as well as sterile neutrinos.  $r_1$  and  $r_2$  are also shown for both cases. The mixing angle  $\vartheta$  has been chosen to be  $45^\circ$ .

$\Delta$ in $10^{-19}$ eV <sup>2</sup>	$M_1$				$r_1$		$M_2$				$r_2$	
	SK		SNO		seq.	st.	SK		SNO		seq.	st.
	seq.	st.	seq.	st.			seq.	st.	seq.	st.		
.0	23.1	23.1	22.5	22.5	1.02	1.02	599.3	599.3	573.0	573.0	1.05	1.05
.3	24.3	25.4	24.3	24.9	1.00	1.02	650.1	696.6	649.7	673.1	1.00	1.03
.6	25.0	26.7	25.5	26.2	.98	1.02	688.8	792.8	712.8	767.7	.97	1.03
.9	25.0	20.0	25.9	19.1	.97	1.05	696.8	504.4	736.2	462.7	.95	1.09
1.2	25.3	17.2	26.4	16.9	.96	1.02	708.8	328.2	764.5	315.1	.93	1.04
1.5	25.5	19.4	26.8	19.1	.95	1.01	719.8	400.0	786.5	390.4	.92	1.02
1.8	25.4	21.9	26.6	21.6	.95	1.02	717.1	518.0	781.9	503.5	.92	1.03
2.1	25.0	23.8	25.8	23.4	.97	1.02	696.6	619.2	742.1	598.7	.94	1.03
2.4	24.5	24.9	24.7	24.3	.99	1.02	666.8	685.1	682.4	658.3	.98	1.04
2.7	24.1	25.1	24.0	24.4	1.00	1.03	643.6	708.1	637.9	676.0	1.01	1.05
3.0	24.0	24.6	24.0	23.9	1.00	1.03	638.8	688.9	633.0	654.4	1.01	1.05
3.5	24.6	22.8	25.1	22.2	.98	1.03	666.8	596.8	690.7	567.2	.97	1.05
4.0	25.2	21.6	26.2	21.2	.96	1.02	702.7	521.0	754.2	500.5	.93	1.04
4.5	25.4	22.0	26.5	21.5	.96	1.02	714.5	531.2	773.3	512.0	.92	1.04
5.0	25.0	23.2	25.9	22.6	.97	1.02	697.4	594.9	742.4	570.7	.94	1.04
5.5	24.6	24.0	25.0	23.4	.98	1.03	669.6	647.8	691.3	619.2	.97	1.05
6.0	24.3	23.8	24.6	23.1	.99	1.03	653.3	642.9	664.3	612.4	.98	1.05
6.5	24.4	22.8	24.9	22.2	.98	1.03	662.4	596.6	684.3	567.5	.97	1.05
7.0	25.1	23.0	26.0	22.6	.97	1.02	696.1	587.8	739.8	564.6	.94	1.04
7.5	25.2	22.3	26.1	21.8	.96	1.02	703.2	555.3	753.6	532.8	.93	1.04

Table 8: Range of variation of  $M_1$ ,  $M_2$ ,  $M_3$ ,  $r_1$ ,  $r_2$  and  $r_3$  for post-bounce epoch neutrinos in the absence of oscillations obtained by changing the input spectra  $f^e(E)$ ,  $\bar{f}^e(E)$ , and  $f^x(E)$ . The symbol + (−) indicates an increase (decrease) of the corresponding spectrum by 30% while 0 signifies the unchanged spectrum.

$f^e(E)$	$\bar{f}^e(E)$	$f^x(E)$	$M_1$		$r_1$	$M_2$		$r_2$
			SK	SNO		SK	SNO	
0	0	0	23.09	22.53	1.02	599.26	572.97	1.05
+	+	−	23.09	22.53	1.02	599.26	572.97	1.05
+	−	−	23.05	21.70	1.06	597.57	534.95	1.12
+	−	+	23.05	21.70	1.06	597.57	534.95	1.12
−	+	+	23.12	23.37	0.99	600.18	610.98	0.98
−	+	−	23.12	23.37	0.99	600.18	610.98	0.98
−	−	+	23.09	22.53	1.02	599.26	572.97	1.05

Table 9:  $R_{SNO}$  for post-bounce epoch neutrinos as a function of the mass splitting  $\Delta$  for  $\vartheta = 15^\circ$  and  $45^\circ$ . Results are presented for oscillation to sequential as well as sterile neutrinos.

$\Delta$ in $10^{-19} \text{ eV}^2$	$R_{SNO}$			
	$\vartheta = 15^\circ$		$\vartheta = 45^\circ$	
	sequential	sterile	sequential	sterile
.0	1.929	1.929	1.929	1.929
.3	1.952	2.050	2.024	2.584
.6	1.894	2.212	1.796	4.837
.9	1.796	2.247	1.488	6.007
1.2	1.749	2.201	1.368	4.565
1.5	1.765	2.145	1.406	3.552
1.8	1.817	2.108	1.549	3.101
2.1	1.876	2.093	1.733	2.945
2.4	1.915	2.094	1.876	2.951
2.7	1.923	2.104	1.908	3.055
3.0	1.905	2.118	1.836	3.211
3.5	1.850	2.139	1.647	3.469
4.0	1.814	2.145	1.539	3.555
4.5	1.818	2.137	1.552	3.444
5.0	1.851	2.125	1.652	3.292
5.5	1.882	2.119	1.753	3.219
6.0	1.881	2.116	1.751	3.186
6.5	1.856	2.118	1.667	3.210
7.0	1.844	2.143	1.628	3.523
7.5	1.830	2.136	1.585	3.430

Table 10: Range of variation of  $R_{SNO}$  for post-bounce epoch neutrinos in the absence of oscillations obtained by changing the input spectra  $f^e(E)$ ,  $\bar{f}^e(E)$ , and  $f^x(E)$ . The symbol + (−) indicates an increase (decrease) of the corresponding spectrum by 30% for case (a) and 10% for case (b) while 0 signifies the unchanged spectrum.

$f^e(E)$	$\bar{f}^e(E)$	$f^x(E)$	$R_{SNO}$	
			Case (a)	Case (b)
			$\pm 30\%$	$\pm 10\%$
0	0	0	1.93	1.93
+	+	−	1.29	1.68
+	−	−	1.48	1.78
+	−	+	2.32	2.06
−	+	+	2.37	2.08
−	+	−	1.54	1.80
−	−	+	3.12	2.24

## Figure Captions

Fig. 1: Contours of constant  $M_1$  for solar neutrinos in the  $\Delta-\vartheta$  plane. (a) and (b) correspond to oscillation to sequential and sterile neutrinos respectively at SK while (c) corresponds to SNO where the two scenarios give identical results.

Fig. 2: The variables (a)  $r_1$ , (b)  $r_2$ , and (c)  $r_3$  for solar neutrinos as a function of the mass splitting  $\Delta$  for two values of the mixing angle  $\vartheta = 45^\circ$  and  $15^\circ$ . The solid (broken) curves correspond to oscillation to sequential (sterile) neutrinos.

Fig. 3: Contours of constant  $r_2$  for solar neutrinos in the  $\Delta-\vartheta$  plane. (a) and (b) correspond to oscillation to sequential and sterile neutrinos respectively. In the absence of oscillation  $r_2 = 0.83$ .

Fig. 4: Contours of constant  $r_3$  for solar neutrinos in the  $\Delta-\vartheta$  plane. (a) and (b) correspond to oscillation to sequential and sterile neutrinos respectively. In the absence of oscillation  $r_3 = 0.78$ .

Fig. 5: Contours of constant  $R_{SNO}$  in the  $\Delta - \vartheta$  plane for oscillation of solar neutrinos to sequential neutrinos. In the absence of oscillation  $R_{SNO} = 0.38$ .

Fig. 6: The variables (a)  $r_1$ , (b)  $r_2$ , and (c)  $r_3$  for collapse phase neutrinos as a function of the mass splitting  $\Delta$  for two values of the mixing angle  $\vartheta = 45^\circ$  and  $15^\circ$ . The solid (broken) curves correspond to oscillation to sequential (sterile) neutrinos.

Fig. 7: Contours of constant  $R_{SNO}$  in the  $\Delta - \vartheta$  plane for oscillation of collapse phase neutrinos to sequential neutrinos. In the absence of oscillation  $R_{SNO} = 0.43$ .

Fig. 8: The variables (a)  $r_1$ , (b)  $r_2$ , and (c)  $r_3$  for post-bounce epoch neutrinos as a function of the mass splitting  $\Delta$  for two values of the mixing angle  $\vartheta = 45^\circ$  and  $15^\circ$ . The solid (broken) curves correspond to oscillation to sequential (sterile) neutrinos.

Fig. 9: Contours of constant  $r_2$  for post-bounce epoch neutrinos in the  $\Delta-\vartheta$  plane. (a) and (b) correspond to oscillation to sequential and sterile neutrinos respectively. In the absence of oscillation  $r_2 = 1.05$ .

Fig. 10: Contours of constant  $R_{SNO}$  in the  $\Delta - \vartheta$  plane for oscillation of post-bounce epoch neutrinos to sterile neutrinos. In the absence of oscillation  $R_{SNO} = 1.93$ .

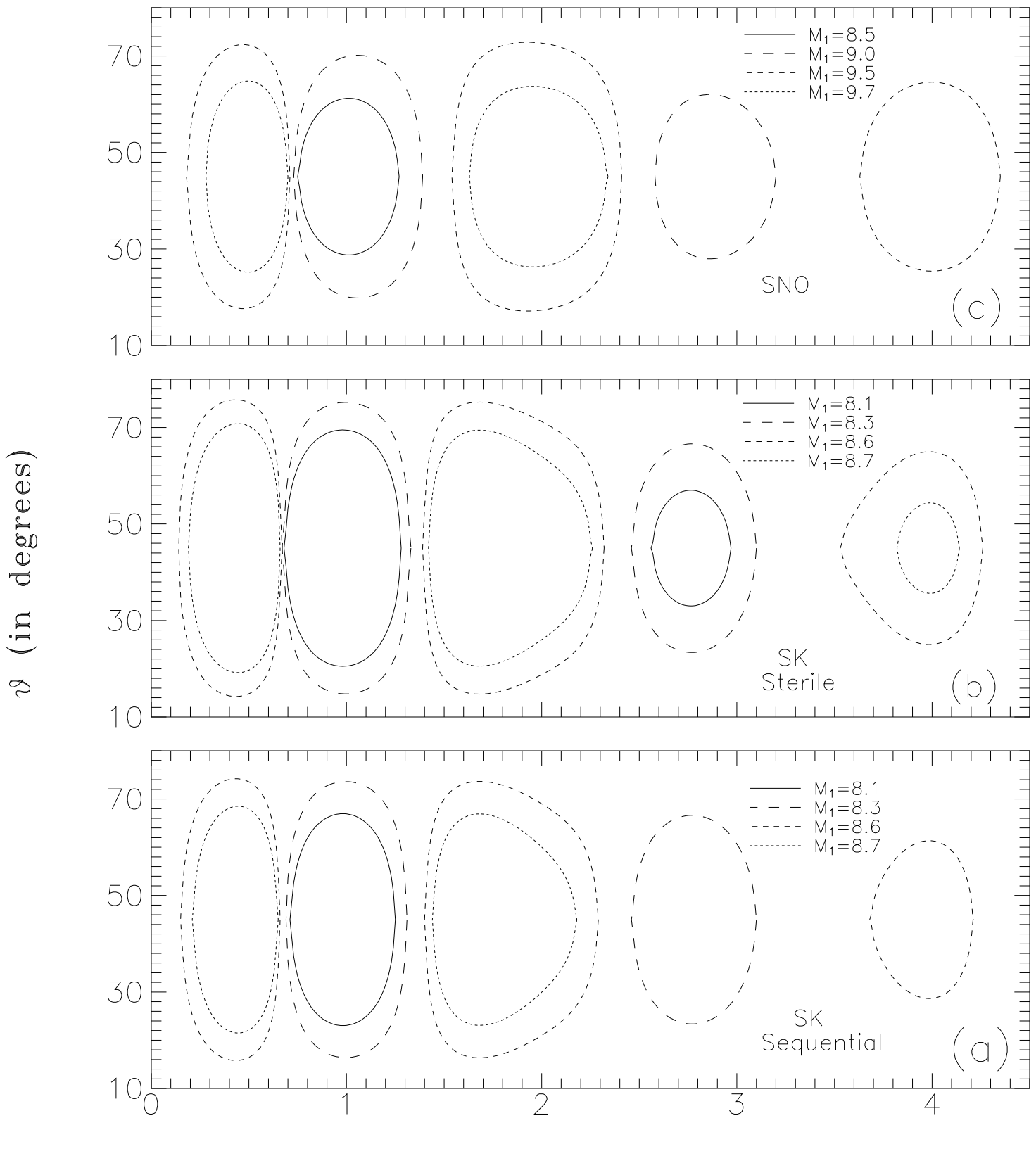


Fig. 1

$\Delta$  (in  $10^{-10} \text{ eV}^2$ )

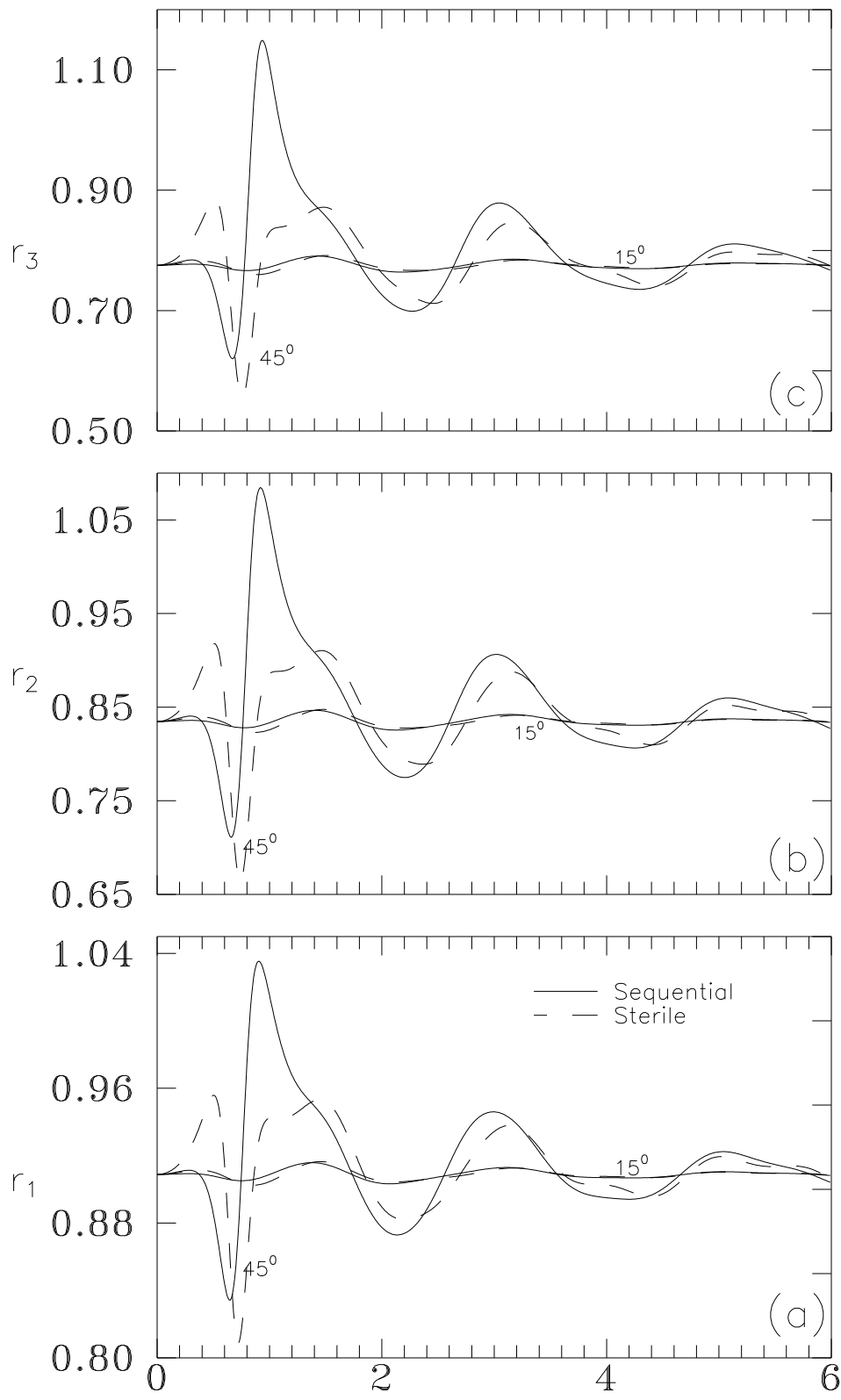


Fig. 2

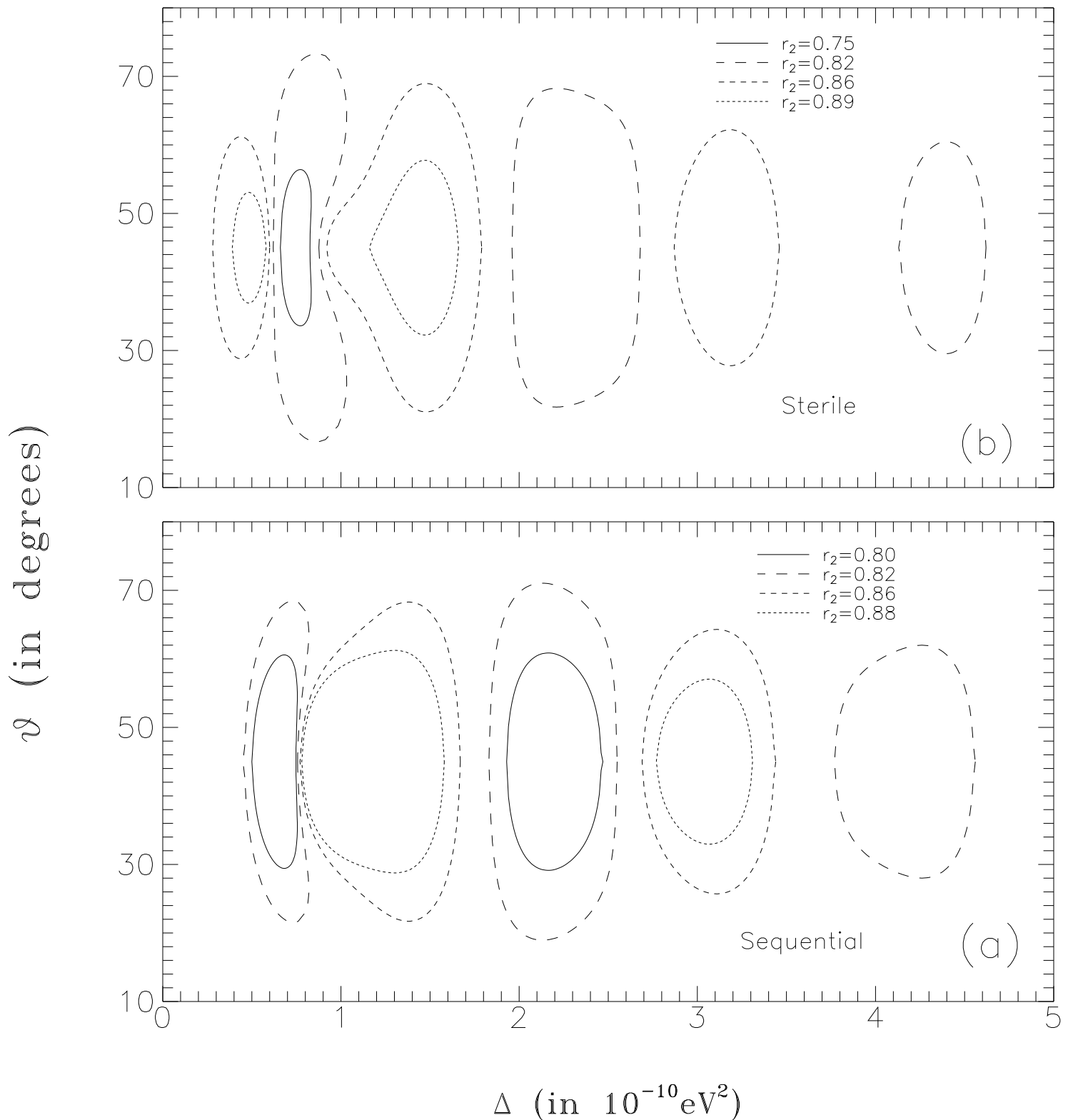


Fig. 3

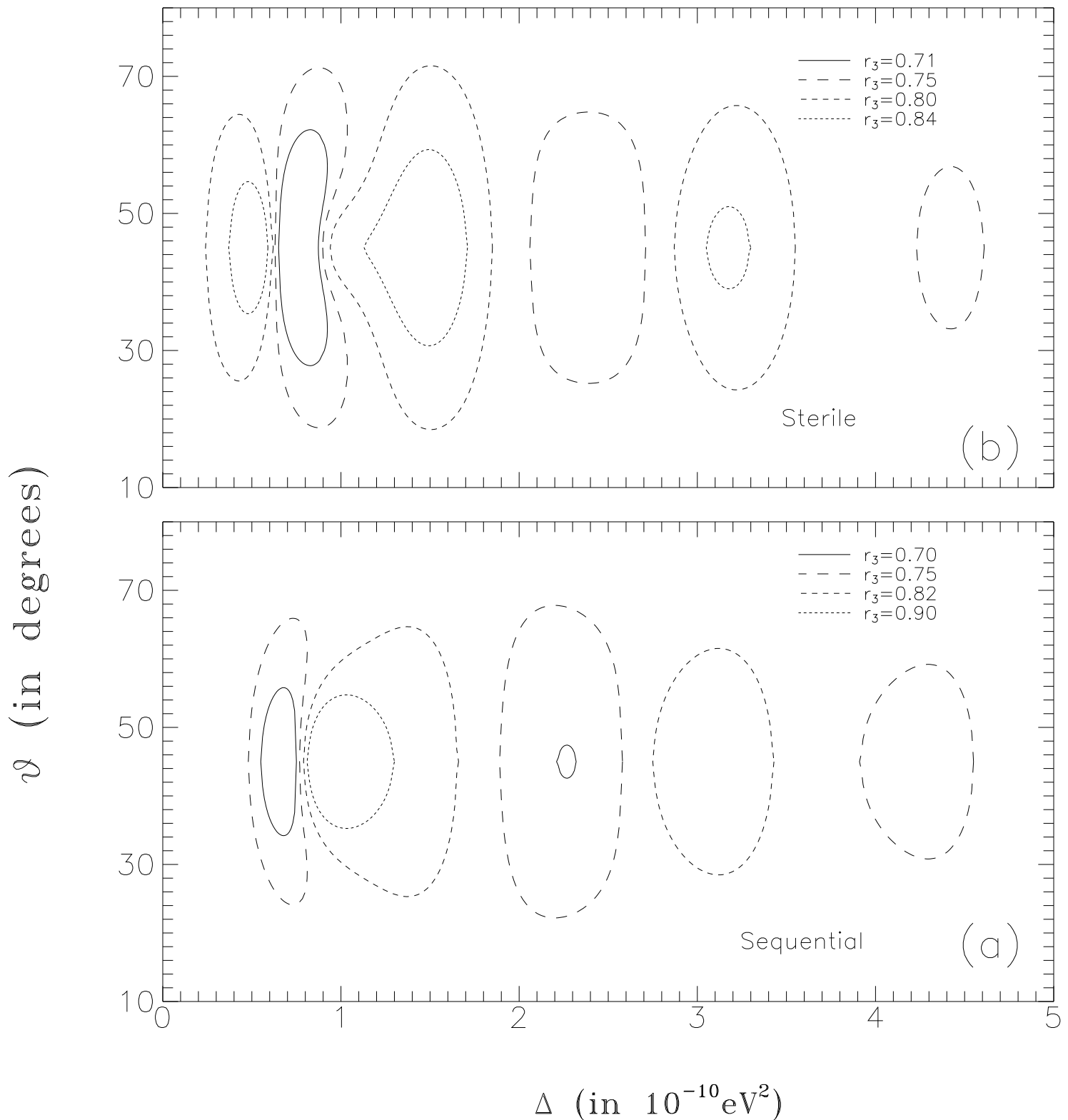


Fig. 4

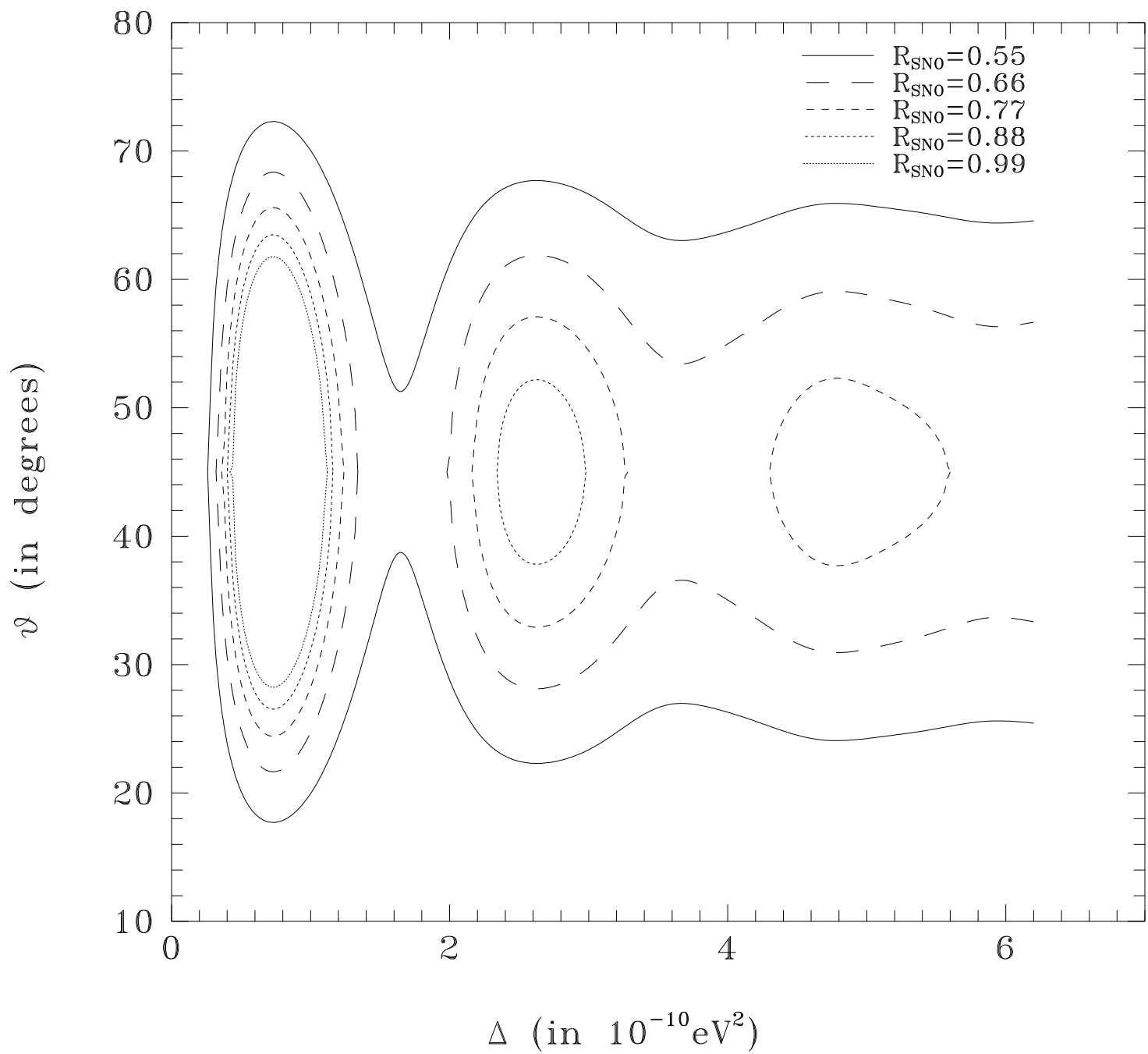


Fig. 5

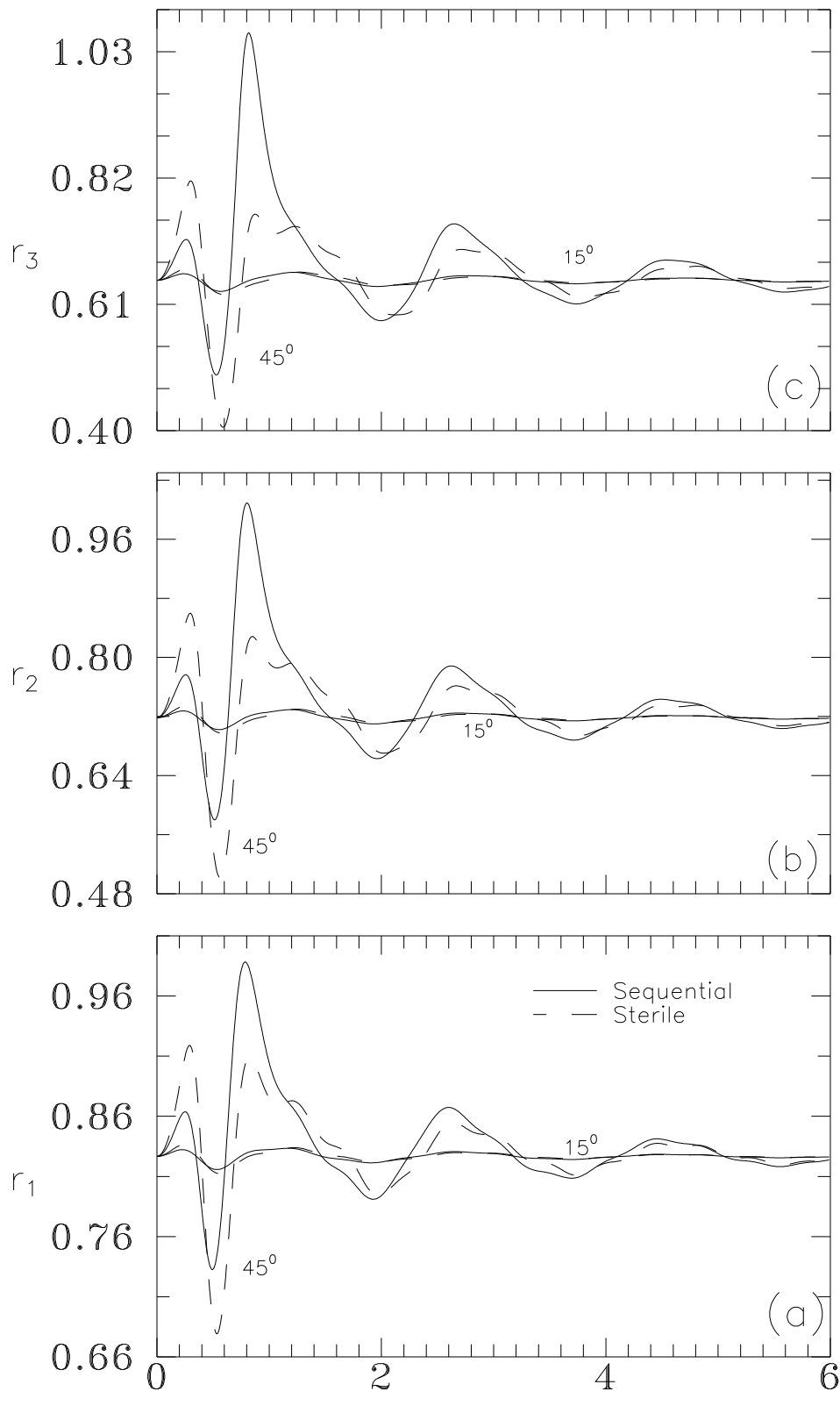


Fig. 6

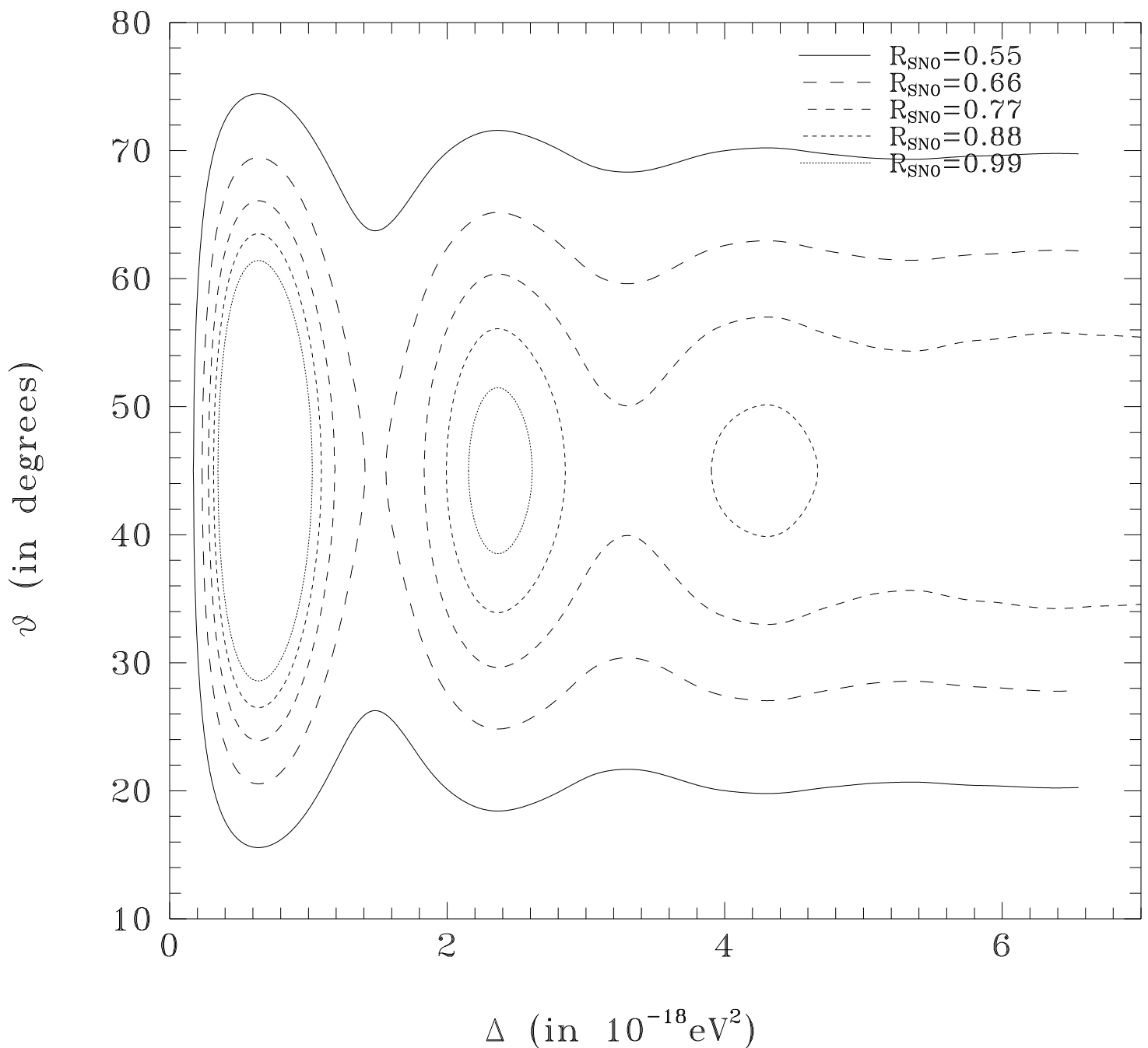


Fig. 7

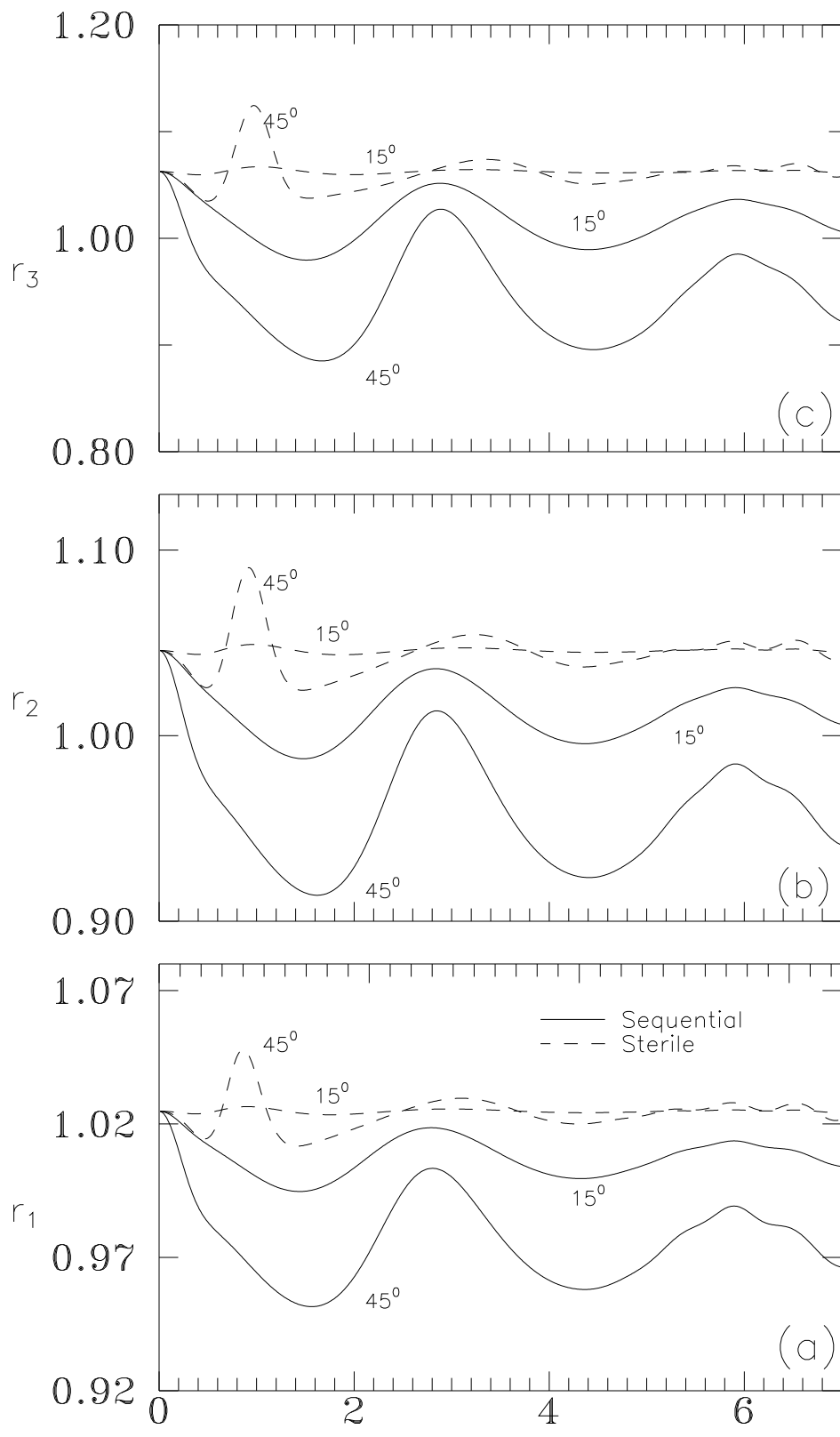


Fig. 8

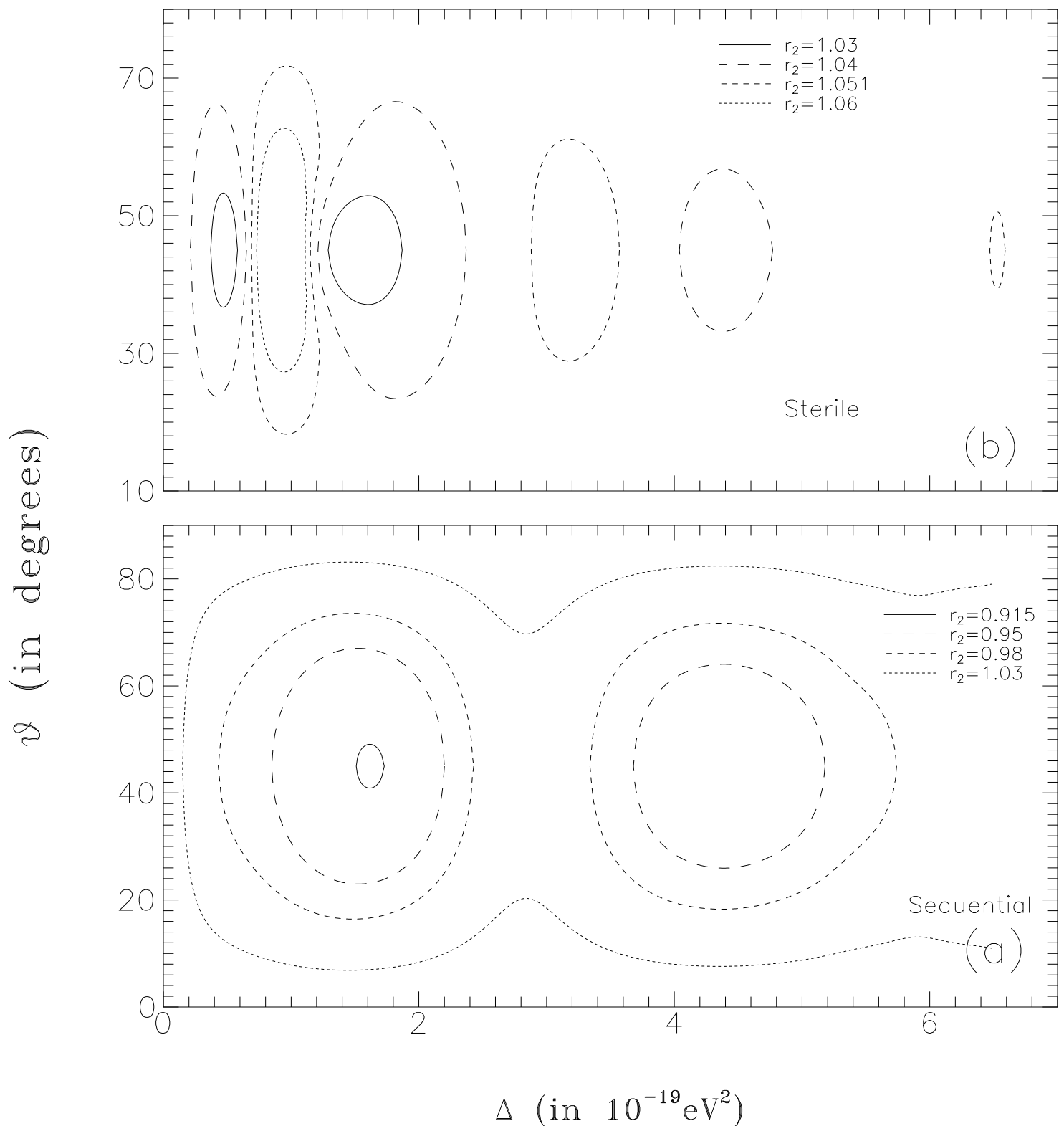


Fig. 9

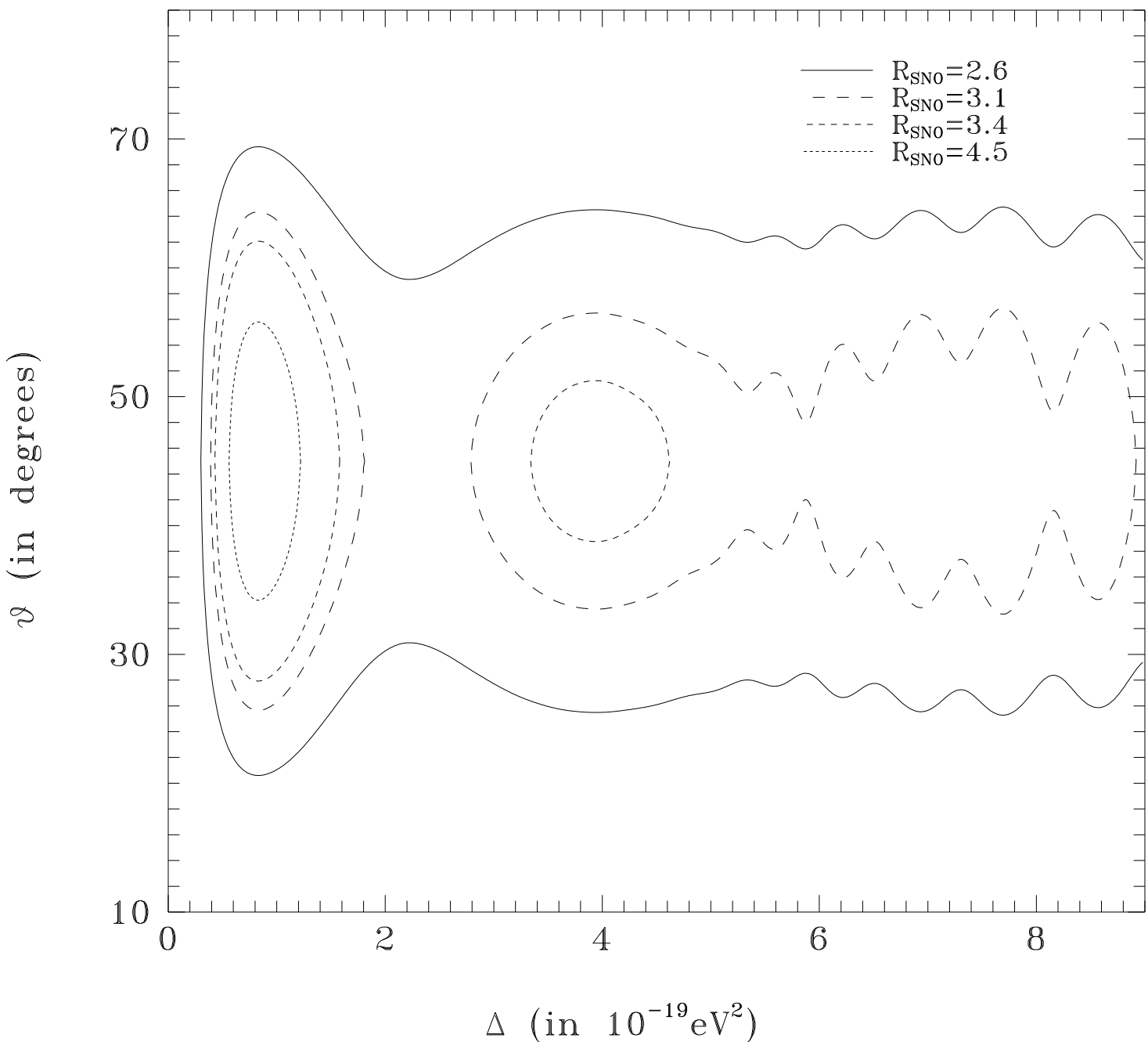


Fig. 10